ACTA MECHANICA SOLIDA SINICA, Vol.13, No.4, December 2000 ISSN 0894 - 9166
Published by HUST, Wuhan, China

MODE I CRACK TIP FIELD WITH STRAIN GRADIENT EFFECTS*

Chen Shaohua Wang Tzuchiang
(*LNM, Institute of Mechanics, Chinese Academy of Sciences, Beijing* 100080, *China*)

ABSTRACT A plane strain mode I crack tip field with strain gradient effects is investigated. A new strain gradient theory is used. An elastic-power law hardening strain gradient material is considered and two hardening laws, i.e. a separation law and an integration law are used respectively. As for the material with the separation law hardening, the angular distributions of stresses are consistent with the HRR field, which differs from the stress results[19]; the angular distributions of couple stresses are the same as the couple stress results[19]. For the material with the integration law hardening, the stress field and the couple stress field can not exist simultaneously, which is the same as the conclusion[19], but for the stress dominated field, the angular distributions of stresses are consistent with the HRR field; for the couple stress dominated field, the angular distributions of couple stresses are consistent with those in Ref.[19]. However, the increase in stresses is not observed in strain gradient plasticity because the present theory is based on the rotation gradient of the deformation only, while the crack tip field of mode I is dominated by the tension gradient, which will be shown in another paper.

KEY WORDS crack tip, stress field, couple stress field, strain gradient effect

I. INTRODUCTION

Many experiments have shown that materials display strong size effects when the characteristic length scale associated with non-uniform plastic deformation is on the order of microns[1-8].

The classical plasticity theories can not predict this size dependence of material behavior at the micron scale because their constitutive models possess no internal length scale.

In order to explain the size effect, it is necessary to develop a continuum theory for the micron level. Fleck and Hutchinson[9] developed a phenomenological theory and a material length scale was introduced for dimensional purposes. While explaining experimental findings of indentation[2,4,10], fracture[11], it has been found necessary to introduce two length parameters[10,12]. One is the length, l_R, that refers to rotational gradients as originally proposed in connection with the torsion measurements and the other, l_S, which refers to stretch gradients. The latter is needed to rationalize length scale phenomena found in indentation and fracture. In 1998, Nix and Gao[13] started from the Taylor relation and gave a kind of hardening law for gradient plasticity. Using the law, they derived the relation between the indentation hardness H and the depth of indentation which could show excellent agreement with the experiment results[5]. Motivated by the indentation hardening law, Gao, Huang et al.[14] pro-

* Supported by the National Natural Science Foundation of China (No.19704100), Science Foundation of Chinese Academy of Sciences (Project KJ951-1-20), CAS K.C.Wong Post-doctoral Research Award Fund and the Post Doctoral Science Fund of China.
Received 19 June 2000.

posed a mechanism-based theory of strain gradient plasticity (MSG). In contrast, no work conjugate of strain gradient has been defined in the alternative gradient theories[15,16], which represent the strain gradient effects as terms relative to Laplacian of effective strain. Retaining the essential structure of conventional plasticity and obeying thermodynamic restrictions, Acharya and Bassani[17] conclude that the only possible formulation is a flow theory with strain gradient effects represented as an internal variable, which acts to increase the current tangent-hardening modulus. However, there has been no systematic way of constructing the tangent modulus to validate this framework. In 2000, Chen and Wang[18] developed this idea and established a systematic way to validate this framework.

Owing to the crack tip singularity, strain gradient effects are important near a crack tip. There is limited progress in applying strain gradient plasticity to the estimation of crack tip fields[19-21]. Reference [19] investigated the mode Ⅰ near tip fields in elastic as well as elastic-plastic materials with strain gradient effects. They showed that stresses and couple stresses near a crack tip can not have the same order of singularity. The near tip field is either stress dominated (stresses are more singular than couple stresses) or couple stress dominated (couple stresses are more singular than stresses). Reference [21] presented a finite element study as well as an asymptotic analysis for mode Ⅰ and mode Ⅱ crack tip fields in strain gradient plasticity. Their asymptotic solution and the finite element analysis also confirmed that stresses and couple stresses near a crack tip do not have the same order of singularity. A common disadvantage to the finite element calculation in all references is that the calculation result is sensitive to the finite formulation.

The aim of the present paper is to investigate the near-tip fields for a crack in elastic-plastic materials with strain gradient effects under mode Ⅰ loading and a new strain gradient plasticity theory is used, in which three rotational degrees of freedom ω_i are introduced in addition to the conventional three translational degrees of freedom u_i, ω_i being not directly dependent upon u_i. The strain energy density is assumed to be a function of the strain tensor and the curvature tensor, and the anti-symmetric part of Cauchy stress vanishes. Two kinds of expressions of strain energy density are used to analyze the crack tip fields respectively. We will start with a new strain gradient plasticity theory for plane strain in Section 2. The near tip fields in elastic-plastic material with strain gradient effects are investigated in Sections 3 and 4. A discussion is given is Section 5.

Ⅱ. THE NEW STRAIN GRADIENT PLASTICITY THEORY

A new strain gradient theory of plasticity is proposed within the framework of general couple stress theory[22], in which three rotational degrees of freedom ω_i are introduced in addition to the conventional three translational degrees of freedom u_i, ω_i being not directly dependent upon u_i, which enables the use of C_0 continuous elements in a finite element formulation. This will be very helpful to the finite element calculation to avoid dramatic sensitivity to the element formulation.

The strain energy density w is assumed to depend only upon the strain tensor $\boldsymbol{\varepsilon}$ and the curvature tensor $\boldsymbol{\chi}$, i.e. the relative rotation tensor $\boldsymbol{\alpha}$ has no contribution to the strain energy density w. It follows that

$$\tau_{ij} = \frac{\partial w}{\partial \alpha_{ij}} = 0 \tag{1}$$

where τ_{ij} is the anti-symmetrical part of Cauchy stress in the general couple stress theory.

The equilibrium equations for stress and couple stress in the body are

$$\sigma_{ij,j} = 0, \qquad m_{ij,j} = 0 \tag{2}$$

The traction boundary conditions for force and moment are

$$\sigma_{ij}n_j = T_i^0, \quad \text{on} \quad S_T \tag{3}$$

$$m_{ij}n_j = q_i^0, \quad \text{on} \quad S_q \tag{4}$$

The additional boundary conditions are

$$u_i = u_i^0, \quad \text{on} \quad S_u \tag{5}$$

$$\omega_i = \omega_i^0, \quad \text{on} \quad S_\omega \tag{6}$$

The deviatoric part s_{ij} of Cauchy stress and deviatoric part m_{ij}' of couple stress are defined as the work conjugates of ε_{ij}', χ_{ij}', respectively; σ_m and m_m are defined as the work conjugates of ε_m and χ_m, respectively, giving

$$\delta w = s_{ij}\delta\varepsilon_{ij}' + m_{ij}'\delta\chi_{ij}' + \sigma_m\delta\varepsilon_m + m_m\delta\chi_m \tag{7}$$

where $s_{ij} \equiv \sigma_{ij} - (1/3)\delta_{ij}\sigma_{kk}$ and $m_{ij}' \equiv m_{ij} - (1/3)\delta_{ij}m_{kk}$.

The above equation enables one to determine s_{ij}, m_{ij}', σ_m and m_m in terms of the strain and curvature states of the solid as

$$s_{ij} = \frac{\partial w}{\partial \varepsilon_{ij}'}, \quad m_{ij}' = \frac{\partial w}{\partial \chi_{ij}'}, \quad \sigma_m = \frac{\partial w}{\partial \varepsilon_m}, \quad m_m = \frac{\partial w}{\partial \chi_m} \tag{8}$$

For a plane strain problem, the nonzero in-plane stresses and couple stresses in polar coordinates are σ_{rr}, $\sigma_{r\theta}(\sigma_{\theta r})$, $\sigma_{\theta\theta}$, m_{zr}, $m_{z\theta}$. The field equations for the equilibrium in 2D are given explicitly in polar coordinates, where the polar coordinates (r, θ) are centered at the crack tip (Fig.1)

$$\begin{cases} \dfrac{\partial \sigma_{rr}}{\partial r} + \dfrac{1}{r}\dfrac{\partial \sigma_{\theta r}}{\partial \theta} + \dfrac{\sigma_{rr} - \sigma_{\theta\theta}}{r} = 0 \\ \dfrac{\partial \sigma_{r\theta}}{\partial r} + \dfrac{1}{r}\dfrac{\partial \sigma_{\theta\theta}}{\partial \theta} + \dfrac{2\sigma_{r\theta}}{r} = 0 \end{cases} \tag{9}$$

$$\frac{\partial m_{zr}}{\partial r} + \frac{1}{r}\frac{\partial m_{z\theta}}{\partial \theta} + \frac{m_{zr}}{r} = 0 \tag{10}$$

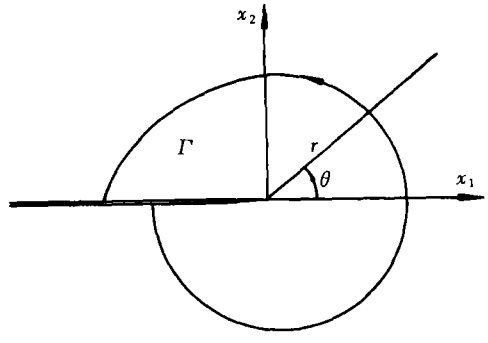

Fig.1 Schematic diagram of a crack and contour of path-independent J integral.

The relations between strains ε_{ij} and displacements u_i are

$$\varepsilon_{rr} = \frac{\partial u_r}{\partial r}, \quad \varepsilon_{\theta\theta} = \frac{1}{r}\frac{\partial u_\theta}{\partial \theta}, \quad \varepsilon_{r\theta} = \varepsilon_{\theta r} = \frac{1}{2}\left(\frac{1}{r}\frac{\partial u_r}{\partial \theta} + \frac{\partial u_\theta}{\partial r} - \frac{u_\theta}{r}\right) \tag{11}$$

The relations between the rotation vector ω_i and curvature tensor χ_{ij} are

$$\chi_{zr} = \frac{\partial \omega_z}{\partial r}, \quad \chi_{z\theta} = \frac{1}{r}\frac{\partial \omega_z}{\partial \theta} \tag{12}$$

The compatibility equations of strain and curvature tensor are as follows:

$$\frac{\partial^2 \varepsilon_{rr}}{\partial \theta^2} - r\frac{\partial \varepsilon_{rr}}{\partial r} - 2\frac{\partial^2 (r\varepsilon_{r\theta})}{\partial r \partial \theta} + \frac{\partial}{\partial r}\left(r^2\frac{\partial \varepsilon_{\theta\theta}}{\partial r}\right) = 0 \tag{13}$$

$$\frac{\partial \chi_{zr}}{\partial \theta} - \frac{\partial (r\chi_{z\theta})}{\partial r} = 0 \tag{14}$$

For an elastic power law hardening material with strain gradient effects, similar to the strain energy density suggested by Ref.[9], we take the strain energy density as

$$w = \frac{n}{n+1}\sigma_0(\varepsilon_e^2 + l^2\chi_e^2)^{(n+1)/(2n)} + \frac{1}{2}K\varepsilon_m^2 + \frac{1}{2}K_1 l^2 \chi_m^2 \tag{15}$$

where n is the hardening power, σ_0 is identified with a measure of the tensile yield stress, $K = E/(3$

$-6\nu)$ is the bulk modulus, K_1 is the bend-torsion bulk modulus, and E and ν are Young's modulus and Poisson's ratio, respectively. It is called the integration law of hardening because ε_e and $l\chi_e$ are coupled together inside the power.

It is pointed out in Ref.[19] that, for an elastic power law hardening material with strain gradient effects, there is another possible expansion for the strain energy density in terms of the invariants of strains and curvatures. Similar to the strain energy density[19], we take another expression of strain energy density

$$w = \frac{n}{n+1}\sigma_0[\varepsilon_e^{(n+1)/n} + (l\chi_e)^{(n+1)/n}] + \frac{1}{2}K\varepsilon_m^2 + \frac{1}{2}K_1 l^2 \chi_m^2 \tag{16}$$

It is called the separation law of hardening because contributions to w from ε_e and $l\chi_e$ are separated.

Equilibrium Eqs.(9) and (10), compatibility Eqs.(13) and (14), and constitutive law (8) provide field equations for the asymptotic analysis near a crack tip in materials with strain gradient effects.

Ⅲ. AN ELASTIC-PLASTIC MATERIAL WITH STRAIN GRADIENT EFFECTS: SEPARATION LAW OF HARDENING

Mode Ⅰ crack tip fields in an elastic-plastic strain gradient material with the separation law of hardening are investigated in this section. The following method is similar to Ref.[19], in which William's expansion is adopted, and is suitable for the dominant as well as higher order asymptotic analyses.

The constitutive relation can be obtained from Eqs.(8) and (16),

$$\varepsilon_{ij} = \frac{3}{2}\left(\frac{\sigma_e}{\sigma_0}\right)^{n-1}\frac{s_{ij}}{\sigma_0} + \frac{1}{9K}\sigma_{kk}\delta_{ij} \tag{17}$$

$$\chi_{ij} = \frac{3}{2}\left(\frac{m_e}{\sigma_0 l}\right)^{n-1}\frac{m_{ij}'}{\sigma_0 l^2} + \frac{1}{9K_1 l^2}m_{kk}\delta_{ij}, \qquad k = r,\theta,z \tag{18}$$

where $\sigma_e^2 = 3(s_{rr}s_{rr} + s_{\theta\theta}s_{\theta\theta} + 2s_{r\theta}s_{r\theta} + s_{zz}^2)/2$ and $m_e^2 = 3(m_{zr}m_{zr} + m_{z\theta}m_{z\theta})/2$ are the Von Mises effective stress and effective couple stress, respectively.

Following Refs.[23,24], the asymptotic stress and couple stress fields near a crack tip can be written as

$$\sigma_{ij}(r,\theta) = \sigma_{ij}^{(0)}(\theta)r^p + O(r^p) \tag{19}$$

$$m_{z\alpha}(r,\alpha) = m_{z\alpha}^{(0)}(\theta)r^p + O(r^p), \qquad \alpha = r,\theta \tag{20}$$

where the power p and angular functions $\sigma_{ij}^{(0)}(\theta)$ and $m_{z\alpha}^{(0)}(\theta)$ are to be determined.

Similar to the classical HRR field[23,24], it has been shown for a power law hardening solid that path independence of J-integral can be expressed as

$$J = \int_\Gamma (wn_1 - T_i u_{i,1} - q_i\omega_{i,1})\mathrm{d}S = \int_\Gamma (wn_1 - n_j\sigma_{ji}u_{i,1} - n_j m_{ji}\omega_{i,1})\mathrm{d}s \tag{21}$$

then, we can obtain

$$p = \frac{-1}{n+1} \tag{22}$$

Substituting Eqs.(19) and (20) into the constitutive relations Eqs.(17) and (18), we obtain the strain tensors and curvature tensors near the crack tip,

$$\varepsilon_{ij} = \frac{3}{2\sigma_0^n}[\sigma_e^{(0)}(\theta)]^{n-1}s_{ij}^{(0)}(\theta)r^{np} \tag{23}$$

$$\chi_{z\alpha} = \frac{3}{2\sigma_0^n l^{n+1}}[m_e^{(0)}(\theta)]^{n-1} m_{z\alpha}^{(0)}(\theta) r^{np} \tag{24}$$

where $s_{ij}^{(0)}(\theta), \sigma_e^{(0)}(\theta), m_{z\alpha}^{(0)}(\theta), m_e^{(0)}(\theta)$ are angular functions for s_{ij}, σ_e, $m_{z\alpha}$ and m_e, respectively.

Substitution of Eqs.(23) and (24) into compatibility Eqs.(13) and (14) yields the following compatibility equations:

$$\frac{d^2}{d\theta^2}\{[\sigma_e^{(0)}(\theta)]^{n-1}[\sigma_{rr}^{(0)}(\theta) - \sigma_{\theta\theta}^{(0)}(\theta)]\} - 4(np+1)\frac{d}{d\theta}\{[\sigma_e^{(0)}(\theta)]^{n-1}\sigma_{r\theta}^{(0)}(\theta)\} - np(np+2)[\sigma_e^{(0)}(\theta)]^{n-1}[\sigma_{rr}^{(0)}(\theta) - \sigma_{\theta\theta}^{(0)}(\theta)] = 0 \tag{25}$$

$$\frac{d}{d\theta}\{[m_e^{(0)}(\theta)]^{n-1} m_{zr}^{(0)}(\theta)\} - (np+1)[m_e^{(0)}(\theta)]^{n-1} m_{z\theta}^{(0)}(\theta) = 0 \tag{26}$$

Substituting Eqs.(19) and (20) into Eqs.(9) and (10), the equilibrium equations become

$$\sigma'^{(0)}_{r\theta}(\theta) = -(p+1)\sigma_{rr}^{(0)}(\theta) + \sigma_{\theta\theta}^{(0)}(\theta) \tag{27}$$

$$\sigma'^{(0)}_{\theta\theta}(\theta) = -(p+2)\sigma_{r\theta}^{(0)}(\theta) \tag{28}$$

$$m'^{(0)}_{z\theta}(\theta) = -(p+1)m_{zr}^{(0)}(\theta) \tag{29}$$

Equations (25), (27) and (28) for stresses and (26) and (29) for couple stresses are uncoupled and can be solved independently.

The traction free conditions are

$$\sigma_{r\theta}(\pm\pi) = \sigma_{\theta\theta}(\pm\pi) = m_{z\theta}(\pm\pi) = 0 \tag{30}$$

The symmetry condition gives

$$\sigma_{r\theta}(0) = \omega_z(0) = u_\theta(0) = 0 \tag{31}$$

The symmetry conditions at $\theta = 0$ in Eq.(31) can be arranged as

$$\sigma_{r\theta}(0) = m_{zr}(0) = 0 \tag{32}$$

and because of the symmetric conditions, at $\theta = 0$, there are

$$\sigma_{rr}^{(0)\prime}(0) = 0, \qquad \sigma_{\theta\theta}^{(0)\prime}(0) = 0 \tag{33}$$

and from Eq.(27), there is

$$\sigma_{r\theta}^{(0)\prime}(0) = -(p+1)\sigma_{rr}^{(0)}(0) + \sigma_{\theta\theta}^{(0)}(0) \tag{34}$$

We find that in order to solve Eqs.(25), (27) and (28) for the stresses, $\sigma_{rr}^{(0)}, \sigma_{\theta\theta}^{(0)}$ are unknown at $\theta = 0$ and $m_{z\theta}^{(0)}$ is unknown at $\theta = 0$ for solving couple stress equations. The shooting method is used to solve the ordinary differential equations for stresses and couple stresses, respectively.

The numerical results show that the stress field is the same as HRR field, which can be easily found since the stress and the couple stress equations are uncoupled.

The couple stress field can be obtained analytically in the same way as it is obtained in Ref. [19],

$$\begin{bmatrix} m_r \\ m_\theta \end{bmatrix} = r^{-1/(n+1)} A_I^{(0)} \left\{\frac{n^2+1}{2n^2} + \frac{n^2-1}{2n^2}\cos 2[\theta - \varphi(\theta)]\right\}^{1/[2(n+1)]} \begin{bmatrix} \sin\varphi(\theta) \\ \cos\varphi(\theta) \end{bmatrix} \tag{35}$$

$$\varphi(\theta) = \frac{1}{2}\left[\theta - \sin^{-1}\left(\frac{n-1}{n+1}\sin\theta\right)\right] \tag{36}$$

Ⅳ. AN ELASTIC-PLASTIC MATERIAL WITH STRAIN GRADIENT EFFECTS: INTEGRATION LAW OF HARDENING

Mode Ⅰ crack tip field in an elastic-plastic strain gradient material with the integration law of hardening is investigated in this section. The constitutive relation can be obtained from Eqs.(8) and

(15)

$$\varepsilon_{ij} = \frac{3}{2}\left(\frac{\Sigma_e}{\sigma_0}\right)^{n-1}\frac{s_{ij}}{\sigma_0} + \frac{1}{9K}\sigma_{kk}\delta_{ij} \tag{37}$$

$$\chi_{ij} = \frac{3}{2}\left(\frac{\Sigma_e}{\sigma_0}\right)^{n-1}\frac{m_{ij}'}{\sigma_0 l^2} + \frac{1}{9K_1 l^2}m_{kk}\delta_{ij}, \quad k = r,\theta,z \tag{38}$$

where

$$\Sigma_e^2 = \frac{3}{2}[s_{rr}^2 + s_{\theta\theta}^2 + 2s_{r\theta}^2] + \frac{3}{2l^2}[m_{zr}^2 + m_{z\theta}^2] \tag{39}$$

Following Refs.[23,24], the asymptotic stress and couple stress fields near a crack tip can be written as Eqs.(19) and (20). The corresponding strains and curvature tensors can be obtained via constitutive relations (37) and (38),

$$\varepsilon_{ij} = \frac{3}{2\sigma_0^n}[\Sigma_e^{(0)}(\theta)]^{n-1}s_{ij}^{(0)}(\theta)r^{np} \tag{40}$$

$$\chi_{ij} = \frac{3}{2\sigma_0^n l^2}[\Sigma_e^{(0)}(\theta)]^{n-1}m_{ij}^{(0)}(\theta)r^{np} \tag{41}$$

where

$$\Sigma_e^{(0)}(\theta) = \left\{\left[\frac{3}{4}(\sigma_{rr}^{(0)} - \sigma_{\theta\theta}^{(0)})^2 + 3(\sigma_{r\theta}^{(0)})^2\right] + \frac{3}{2l^2}[m_{zr}^{(0)}m_{zr}^{(0)} + m_{z\theta}^{(0)}m_{z\theta}^{(0)}]\right\}^{1/2} \tag{42}$$

and $s_{ij}^{(0)}(\theta)$, $m_{ij}^{(0)}(\theta)$, $\Sigma_e^{(0)}(\theta)$ are angular functions for s_{ij}, m_{ij}, Σ_e, respectively. Substitution of Eqs.(40) and (41) into compatibility Eqs.(13) and (14) gives the following compatibility equations:

$$\frac{d^2}{d\theta^2}[(\Sigma_e^{(0)})^{n-1}(\sigma_{rr}^{(0)} - \sigma_{\theta\theta}^{(0)})] - 4(np+1)\frac{d}{d\theta}[(\Sigma_e^{(0)})^{n-1}\sigma_{r\theta}^{(0)}] - np(np+2)(\Sigma_e^{(0)})^{n-1}\cdot(\sigma_{rr}^{(0)} - \sigma_{\theta\theta}^{(0)}) = 0 \tag{43}$$

$$\frac{d}{d\theta}[(\Sigma_e^{(0)})^{n-1}m_{zr}^{(0)}] - (np+1)(\Sigma_e^{(0)})^{n-1}\cdot m_{z\theta}^{(0)} = 0 \tag{44}$$

Substitution of Eq.(42) into Eqs.(43) and (44) gives

$$(n-1)(n-2)(\sigma_{rr}^{(0)} - \sigma_{\theta\theta}^{(0)})\Sigma_e^{(0)\prime} + 2(n-1)\Sigma_e^{(0)}(\sigma_{rr}^{(0)\prime} - \sigma_{\theta\theta}^{(0)\prime})\Sigma_e^{(0)\prime} + (\Sigma_e^{(0)})^2(\sigma_{rr}^{(0)\prime\prime} - \sigma_{\theta\theta}^{(0)\prime\prime}) + (n-1)\Sigma_e^{(0)}(\sigma_{rr}^{(0)} - \sigma_{\theta\theta}^{(0)})\Sigma_e^{(0)\prime\prime} - 4(np+1)[(n-1)\Sigma_e^{(0)}\sigma_{r\theta}^{(0)}\Sigma_e^{(0)\prime} + (\Sigma_e^{(0)})^2\sigma_{r\theta}^{(0)\prime}] - np(np+2)(\Sigma_e^{(0)})^2(\sigma_{rr}^{(0)} - \sigma_{\theta\theta}^{(0)}) = 0 \tag{45}$$

$$(n-1)m_{zr}^{(0)}\Sigma_e^{(0)\prime} + \Sigma_e^{(0)}m_{zr}^{(0)\prime} - (1+np)\Sigma_e^{(0)}m_{z\theta}^{(0)} = 0 \tag{46}$$

where

$$\Sigma_e^{(0)\prime} = \frac{1}{2\Sigma_e^{(0)}}\left\{\frac{3}{2}(\sigma_{rr}^{(0)} - \sigma_{\theta\theta}^{(0)})(\sigma_{rr}^{(0)\prime} - \sigma_{\theta\theta}^{(0)\prime}) + 6\sigma_{r\theta}^{(0)}\sigma_{r\theta}^{(0)\prime} + \frac{3}{l^2}[m_{zr}^{(0)}m_{zr}^{(0)\prime} + m_{z\theta}^{(0)}m_{z\theta}^{(0)\prime}]\right\} \tag{47}$$

$$\Sigma_e^{(0)\prime\prime} = -\frac{1}{4(\Sigma_e^{(0)})^3}\left[\frac{3}{2}(\sigma_{rr}^{(0)} - \sigma_{\theta\theta}^{(0)})(\sigma_{rr}^{(0)\prime} - \sigma_{\theta\theta}^{(0)\prime}) + 6\sigma_{r\theta}^{(0)}\sigma_{r\theta}^{(0)\prime} + \frac{3}{l^2}(m_{zr}^{(0)}m_{zr}^{(0)\prime} + m_{z\theta}^{(0)}m_{z\theta}^{(0)\prime})\right]^2 + \frac{1}{2\Sigma_e^{(0)}}\left\{\frac{3}{2}(\sigma_{rr}^{(0)\prime} - \sigma_{\theta\theta}^{(0)\prime})^2 + \frac{3}{2}(\sigma_{rr}^{(0)} - \sigma_{\theta\theta}^{(0)})(\sigma_{rr}^{(0)\prime\prime} - \sigma_{\theta\theta}^{(0)\prime\prime}) + 6(\sigma_{r\theta}^{(0)\prime})^2 + 6\sigma_{r\theta}^{(0)}\sigma_{r\theta}^{(0)\prime\prime} + \frac{3}{l^2}[(m_{zr}^{(0)\prime})^2 + m_{zr}^{(0)}m_{zr}^{(0)\prime\prime} + (m_{z\theta}^{(0)\prime})^2 + m_{z\theta}^{(0)}m_{z\theta}^{(0)\prime\prime}]\right\} \tag{48}$$

The equilibrium equations are the same as Eqs.(27) – (29).

Unlike the analysis in Section 3, the governing equations for stresses and couple stresses (27) – (29) and (43) – (44) are coupled together through $\Sigma_e^{(0)}(\theta)$ and the equations are differential about $\sigma_{ij}^{(0)\prime\prime}(\theta)$ and $m_{ij}^{(0)\prime\prime}(\theta)$. For a solution by means of numerical calculation, the values of the other components, i.e. $\sigma_{rr}^{(0)}(\theta)$, $\sigma_{\theta\theta}^{(0)}(\theta)$, $m_{z\theta}^{(0)}(\theta)$, $m_{zr}^{(0)\prime}(\theta)$, $m_{z\theta}^{(0)\prime}(\theta)$ at $\theta = 0$ should be initially known except for Eqs.(32) – (34). From Eq.(29), we obtain

$$m_{z\theta}^{(0)\prime}(\theta) = -(p+1)m_{zr}^{(0)}(\theta), \qquad \text{at } \theta = 0 \tag{49}$$

At $\theta = 0$, substituting Eqs.(32) – (34) and (49) into Eq.(47), we obtain

$$\Sigma_e^{(0)\prime}(\theta) = 0, \qquad \text{at } \theta = 0 \tag{50}$$

Substituting Eq.(50) into Eq.(46), the following condition is obtained

$$m_{zr}^{(0)\prime}(0) = (1+np)m_{z\theta}^{(0)}(0) \tag{51}$$

Thus, the values of $\sigma_{rr}^{(0)}(\theta)$, $\sigma_{\theta\theta}^{(0)}(\theta)$, $m_{z\theta}^{(0)}(\theta)$ at $\theta = 0$ are unknown and should be initially guessed and then determined by the crack tip face traction free conditions in Eq.(30). Since all governing equations and boundary conditions are homogeneous, we impose the normalization

$$\sqrt{\sigma_{rr}^{(0)2} + \sigma_{\theta\theta}^{(0)2} + l^{-2}m_{z\theta}^{(0)2}}\Big|_{\theta=0} = \sigma_0 l^{1/(n+1)}$$

where $\sigma_0 l^{1/(n+1)}$ appears only to balance the dimension[20]. This normalization condition can be written as

$$\frac{l^{-1}m_{z\theta}^{(0)}|_{\theta=0}}{\sigma_0 l^{1/(n+1)}} = \cos\phi, \quad \frac{\sigma_{rr}^{(0)}|_{\theta=0}}{\sigma_0 l^{1/(n+1)}} = \sin\phi\cos\psi, \quad \frac{\sigma_{\theta\theta}^{(0)}|_{\theta=0}}{\sigma_0 l^{1/(n+1)}} = \sin\phi\sin\psi$$

$$0 \leqslant \phi \leqslant \pi/2, \qquad 0 \leqslant \psi \leqslant 2\pi \tag{52}$$

For each given ϕ and ψ, the Runge-Kutta method is used to start from initial conditions at $\theta = 0$ and to progress to the crack face $\theta = \pi$. When the numerically calculated angular distribution of stresses and couple stresses meets the crack face traction-free conditions Eq.(30), a near tip asymptotic field is obtained. The success in choosing two parameters ϕ and ψ to meet three boundary conditions in Eq.(30) simultaneously indicates that the power of stress and couple stress singularity in Eq.(22) is correct.

The entire range of ϕ and ψ is discretized into 90×360 grids, i.e., one degree per increment for ϕ and ψ. The above-mentioned shooting method is applied over all grid points. Two solutions are obtained for mode Ⅰ, giving $\phi = \pi/2$ and $\phi = 0$, respectively. One solution corresponds to a stress-dominated near tip field ($\phi = \pi/2$, couple stresses vanishing and the stress dominated field is the same as HRR field), while the other gives a couple stress dominated near tip field ($\phi = 0$, stresses vanishing and the couple stress dominated field is the same as that obtained in Ref.[19] for mode Ⅰ crack tip field). For the two types of near tip fields, the combined measure of effective stress Σ_e becomes the same as the Von Mises stress σ_e and effective couple stress m_e, respectively. However, the two fields can not exist simultaneously near a crack tip in a material with the integration law of hardening.

The angular distribution of stresses and couple stresses are shown in Fig.2 and Fig.3 for the hardening exponent $n = 10$. It is observed for the stress dominated field that the stresses are consistent with those in HRR field, but different from the corresponding components in Ref.[19]. The couple stress dominated field is the same as the couple stress field for the separation law of hardening, i.e. the same as that in Ref.[19] for mode Ⅰ crack tip field.

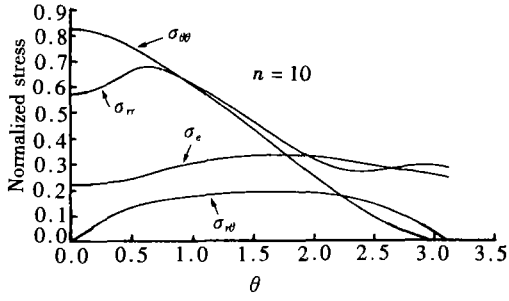

Fig.2 The angular distributions of the normalized stress.

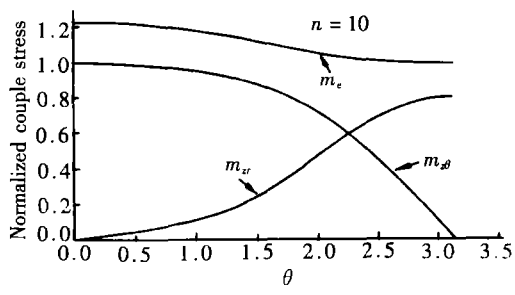

Fig.3 The angular distributions of the normalized couple stress.

V. DISCUSSION

The mode I near tip field for a power law hardening material with strain gradient effects consists of stress field and couple stress field, while the stress field is consistent with HRR field and the couple stress field can be obtained analytically in the same way as the counterpart[19].

The near tip field for the separation law of hardening is the combination of stress dominated field and couple stress dominated field. For the integration law of hardening——stresses, strains and displacements are identical to their counterparts in the stress dominated field, while couple stresses, curvature tensors and rotation tensors are identical to their counterparts in the couple stress dominated field. The structure of the near tip field is insensitive to the choice of separation or integration law of hardening in strain gradient plasticity.

The near tip stress field of mode I obtained by means of the new strain gradient theory is different from that in Ref.[19] since the stress dominated field (the couple stress is less singular and has hardly any contribution to the strain energy)[19] is different from HRR stress field.

The increase, however, is not observed in stresses because the strain gradient plasticity theory used in the present study is based on the rotation gradient of the deformation only and the stress dominated field can not exist simultaneously with the couple stress dominated field.

Further work will be done using the strain gradient theory, in which the stretch gradient effect is considered.

REFERENCES

[1] Lloyd, D.J., Particle reinforced aluminum and magnesium matrix composites, *Int. Mater. Rev.*, Vol.39, 1994, 1 - 23.

[2] Nix, W.D., Mechanical properties of tin films, *Metall. Trans.*, Vol.20A, 1989, 2217 - 2245.

[3] Ma, Q. and Clarke, D.R., Size dependent hardness in silver single crystals, *J. Mater. Res.*, Vol.10, 1995, 853 - 863.

[4] Poole, W.J., Ashby, M.F. and Fleck, N.A., Microhardness of annealed and work-hardened copper polycrystals, *Scripta Metall. Mater.*, Vol.34, 1996, 559 - 564.

[5] McElhaney, K.W., Vlassak, J.J. and Nix, W.D., Determination of indenter tip geometry and indentation contact area for depth-sensing indentation experiments, *J. Mater. Res.*, Vol.13, 1998, 1300 - 1306.

[6] Smyshlyaev, V.P. and Fleck, N.A., The role of strain gradients in the grain size effect for polycrystals, *J. Mech. Phys. Solids*, Vol.44, 1996, 465 - 495.

[7] Fleck, N.A., Muller, G.M., Ashby, M.F. and Hutchinson, J.W., Strain gradient plasticity: theory and experiment, *Acta Metal. et Mater*, Vol.42, 1994, 475 – 487.

[8] Stolken, J.S. and Evans, A.G., A microbend test method for measuring the plasticity length scale, *Acta Mater.*, Vol.46, 1998, 5109 – 5115.

[9] Fleck, N.A. and Hutchinson, J.W., A phenomenological theory for strain gradient effects in plasticity, *J. Mech. Phys. Solids*, Vol.41, 1993, 1825 – 1857.

[10] Begley, M.R. and Hutchinson, J.W., The mechanics of size-dependent indentation, Harvard University Report Mech – 309, Division of Engineering and Applied Sciences, Harvard University, Cambridge, Massachussetts, 1997.

[11] Wei, Y. and Hutchinson, J.W., Steady-state crack growth and work of fracture for solids characterized by strain gradient plasticity, *J. Mech. Phys. Solids*, Vol.45, 1997, 1253 – 1273.

[12] Fleck, N.A. and Hutchinson, J.W., Strain gradient plasticity, Advances in Applied Mechanics ed. J.W. Hutchinson ad T.Y. Wu, Academic Press, New York, 1997, 33:295 – 361.

[13] Nix, W.D. and Gao, H., Indentation size effects in crystalline materials: a law for strain gradient plasticity, *J. Mech. Phys. Solids*, Vol.46, 1998, 411 – 425.

[14] Gao, H., Huang, Y, Nix, W.D. and Hutchinson, J.W., Mechanism-based strain gradient plasticity- Ⅰ. theory, *J. Mech. Phys. Solids*, Vol.47, 1999, 1239 – 1263.

[15] Aifantis, E.C., On the microstructural origin of certain inelastic models, *Trans. ASME J. Eng. Mater. Technol.*, Vol.106, 1984, 326 – 330.

[16] Muhlhaus, H.B. and Aifantis, E.C., The influence of microstructure-induced gradients on the localization of deformation in viscoplastic materials, *Acta Mechanica*, Vol.89, 1991, 217 – 231.

[17] Acharya, A. and Bassani, J.L., On non-local flow theories that preserve the classical structure of incremental boundary value problems, In Micromechanics of Plasticity and Damage of Multiphase Materials, IUTAM Symposium, Paris, Aug 29-Sept 1, 1995.

[18] Chen, S.H. and Wang, T.C., A new hardening law for strain gradient plasticity, Vol.48, No.16, 2000, 3997 – 4005.

[19] Huang, Y., Zhang, L., Guo, T.F. and Huang, K.C., Mixed mode near tip fields for cracks in materials with strain gradient effects, *J. Mech. Phys. Solids*, Vol.45, No.3, 1997, 439 – 465.

[20] Chen, J.Y., Huang, Y. and Huang, K.C., Mode Ⅰ and Mode Ⅱ plane stress near tip fields for cracks in materials with strain gradient effects, Key Engineering Materials, Vols.145 – 149, 1998, 19 – 28.

[21] Xia, Z.C. and Hutchinson, J.W., Crack tip fields in strain gradient plasticity, *J. Mech. Phys. Solids*, Vol.44, 1996, 1621 – 1648.

[22] Cosserat, E. and Cosserat, F., Théorie des Corps Déformables (Herman et fils, Paris), 1909.

[23] Hutchinson, J.W., Singular behavior at the end of a tensile crack in a hardening material, *J. Mech. Phys. Solids*, Vol.16, 1968, 13 – 31.

[24] Rice, J.R. and Rosengren, G.F., Plane strain deformation near a crack tip in a power law hardening material, *J. Mech. Phys. Solids*, Vol.16, 1968, 1 – 12.